

# Introduction of Arc Observation Technologies

Terumichi Cho,  
Kenta Yamamura

**Keywords** High voltage, High capability, VCB, VI, Axial Magnetic Field (AMF)

## Abstract

To realize higher voltage and larger current interruption capability for the Vacuum Circuit-Breaker (VCB), we evaluated the physical properties of the electrode materials of the Vacuum Interrupter (VI). We observed arcs in a vacuum chamber where Axial Magnetic Field (AMF) electrodes are allocated. We did a comparison of performance characteristics by short-circuit test. To pursue higher VI performance, however, it is necessary to carry out quantitative evaluation of current interruption phenomena. For this reason, we added a high-speed two-color radiation pyrometer to our arc observation facility. Since then, it became possible to measure the electrode surface temperature behind the current-zero point and the relationship was clarified among the magnetic field intensity around the AMF electrode, arcing energy, and electrode surface melting conditions. For the reduction of melting conditions at the time of current interruption, it is essential to disperse the generated arcs stably and uniformly by magnetic field intensity.

## 1 Preface

Against recent technical trends toward a higher voltage and a larger current interruption capability of the vacuum circuit breaker, we are currently promoting basic data acquisition for the Axial Magnetic Field (AMF) electrodes. The magnetic field intensity around the AMF electrode is one of the factors that determine the larger current interruption capability. It is, therefore, important to make a quantitative evaluation of the related characteristics.

We introduced a high-speed two-color radiation pyrometer to a conventional arc observation facility and used the AMF electrodes of different magnetic field intensities to measure arc energy generated at the time of high-current interruption and electrode surface temperatures. This paper introduces the examined characteristics.

## 2 AMF Electrode

**Fig. 1** shows the principle of current interruption by AMF electrodes. For the AMF electrode, magnetic fields in parallel to arcs are generated among electrodes at the time of current interruption due to the electrode construction. Since electrons

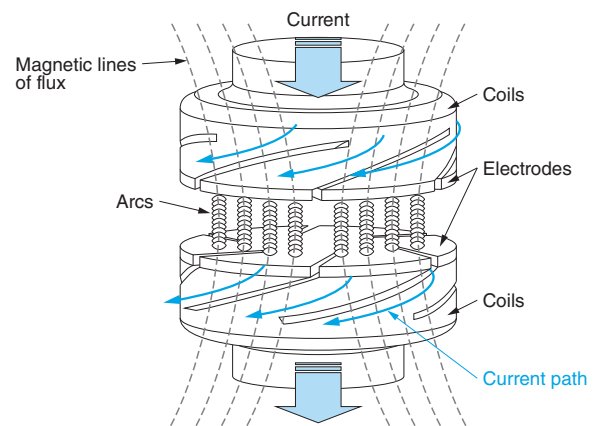


**Fig. 1** Principle of Current Interruption by AMF Electrodes

An outlined construction of the AMF electrodes and principle of current interruption are shown.

and ions are restricted by magnetic flux lines, arcs are uniformly dispersed and local heating around the electrodes is reduced as a result. This principle is utilized to realize high-current interruption.

## 3 Test Conditions

**Fig. 2** shows an arc observing device. The

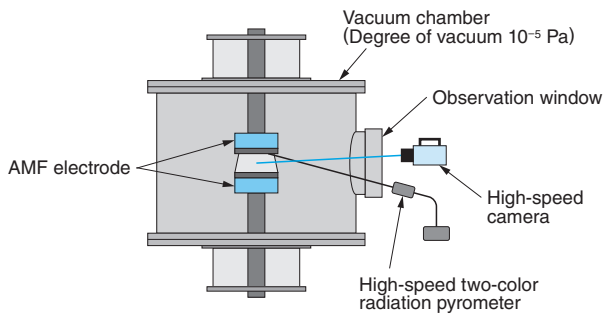


**Fig. 2 Arc Observing Device**

An outlined diagram of the vacuum chamber and measuring devices is shown.

**Table 1 Performance Characteristics of High-Speed Camera**

The performance characteristics of the high-speed camera used for the testing are shown.

Items	Specifications
Photographing speed	210,000 fps
Shutter speed	1/316,984 s
Resolution	384 × 160 px

**Table 2 Performance Characteristics of High-Speed Two-Color Radiation Pyrometer**

The performance characteristics of the high-speed two-color radiation pyrometer used for the testing are shown.

Items	Specifications
Temperature range	650~1800°C
Response speed	0.12 ms
Wavelength band	1.65~1.75 μm 1.75~2.00 μm
Detector device	InGaAs

AMF electrodes made of a copper-chromium alloy material are allocated in a vacuum chamber where the vacuum degree at  $10^{-5}$  Pa is maintained. The AMF electrodes can be observed through an observation window and it is possible to measure the electrode surface temperature at the time of arc generation and after the current-zero point with the aid of a high-speed camera and a high-speed two-color radiation pyrometer. **Table 1** shows the performance characteristics of a high-speed camera and **Table 2** shows the performance characteristics of a high-speed two-color radiation pyrometer.

**Fig. 3** shows the test circuit and **Fig. 4** shows the carried current waveform and CB switching stroke. For testing, a Switch for Resistance (MRSW) is turned on to carry a low current and make the Test

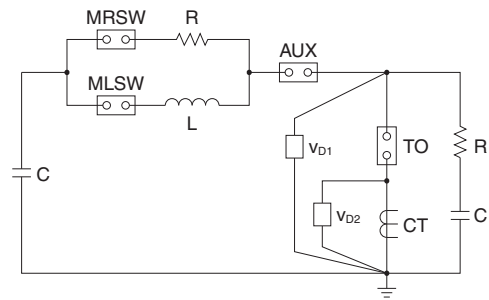


**Fig. 3 Test Circuit**

The test circuit for the arc observing device is shown.

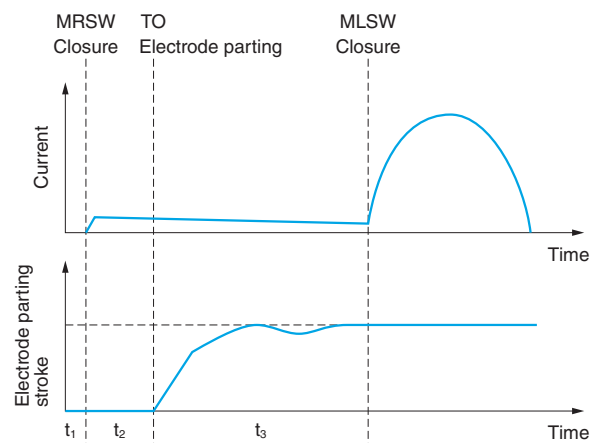


**Fig. 4 Carried Current Waveform and CB Switching Stroke**

Waveform of carried current (upper stage) and that of CB switching stroke (lower stage) are shown.

Object (TO) take a contact parting action. When a complete contact-open condition is assumed, a Switch for Reactor (MLSW) is turned on to carry an AC half-wave current at 50 Hz. The breaking current is adjusted with a capacitor charging voltage.

**Fig. 5** shows the AMF electrode and **Table 3** shows the AMF electrode conditions for testing. The AMF electrode is produced in a process where a copper-chromium alloy electrode with a diameter of 40mm connects with a coil (copper) and a lead (copper) by soldering with the use of a silver alloy brazing filler. The electrode and coil are processed to have three slits equally aligned. The axial magnetic field intensity is regulated to 0.54, 0.80, and 1.00 p.u., respectively, by adjusting the slit length. The magnetic field is calculated with the use of magnetic field analysis. The high-speed two-color radiation pyrometer is used for the measurement at a point shown in **Fig. 5**. This is the region where the magnetic field intensity is strongest in the case of magnetic field analysis.

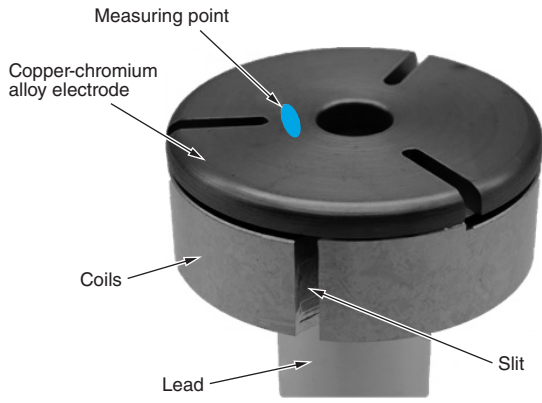


**Fig. 5 AMF Electrode**

The AMF electrode used for the testing is shown.

**Table 3 AMF Electrode Conditions**

The conditions of the AMF electrode used for the testing are shown.

Items	Specifications
Electrode diameter	$\phi 40$
Electrode materials	CuCr
No. of slits	3 (Equally aligned)
Magnetic field intensity (3 kinds)	0.54 p.u. 0.80 p.u. 1.00 p.u.

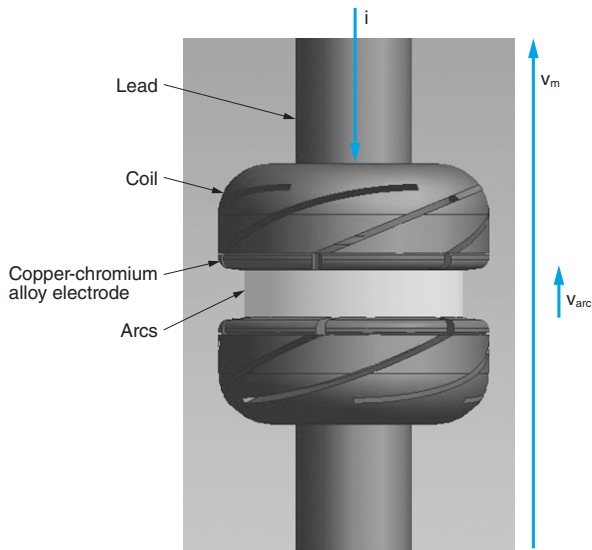


**Fig. 6 Arc Energy Calculation Parameters**

Parameters used for arc energy calculation are shown.

## 4 Arc Energy Calculation Method

Fig. 6 shows the arc energy calculation parameters. The arc energy  $W$  is derived from Expression (1) below, where  $v_{arc}$  is arc voltage,  $i$  is current, and

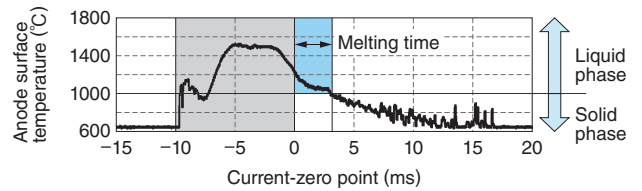
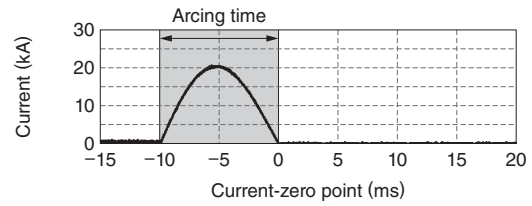


**Fig. 7 Definition of Melting Time**

Definition of the melting time is shown.

$t_{arc}$  is AC arcing time. As shown by Expression (2),  $v_{arc}$  is a value obtained by subtracting the resistance-component voltage of the  $TO$  and the induced voltage from the measured voltage  $v_m$ . The value  $v_m$  is derived from Expression (3) by subtracting the measured voltage on low-voltage  $v_{D2}$  from the measured voltage on high-voltage side  $v_{D1}$ .

$$W = \int_{t_{arc}} i(t) \times v_{arc}(t) dt \quad \dots \quad (1)$$

$$v_{arc}(t) = v_m(t) - R_{TO} i(t) - L_{TO} \frac{di(t)}{dt} \quad \dots \quad (2)$$

$$v_m(t) = v_{D1}(t) - v_{D2}(t) \quad \dots \quad (3)$$

## 5 Definition of Melting Time

Fig. 7 shows the definition of the melting time. The duration from the current-zero point to the time when the anode surface temperature lowers to  $1000^\circ\text{C}$ , which is equivalent to the copper melting point, is defined as the melting time. The resultant values of testing were examined by comparison.

Since arcs are already generated before the time at the current-zero point, temperatures cannot be measured accurately.

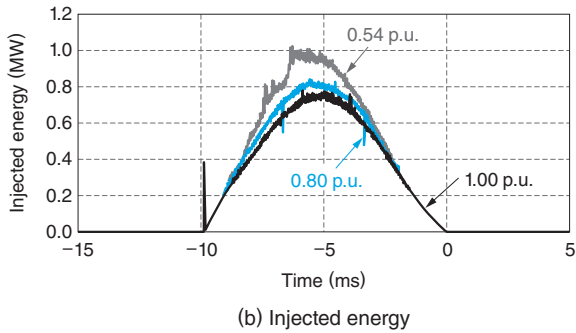
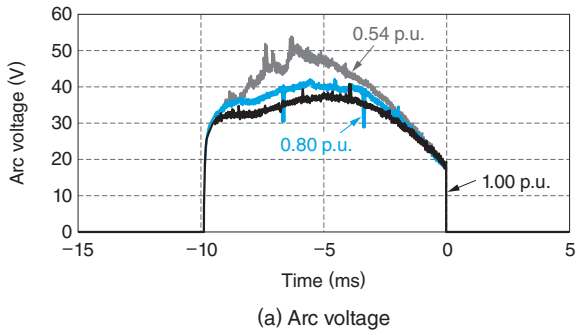
## 6 Test Result

### 6.1 Measurement

Fig. 8 shows examples of measured waveforms.

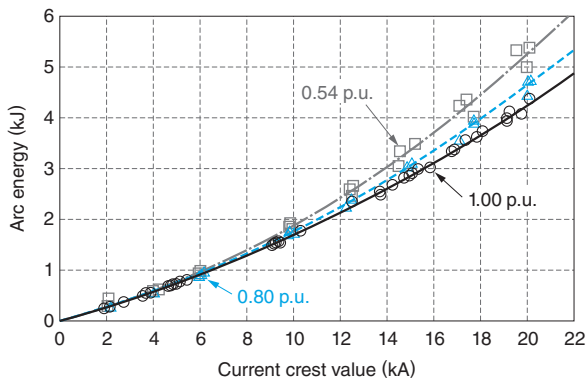
### 6.2 Comparison of Arc Energy Measurement

Fig. 9 shows the relationship between current



**Fig. 8** Examples of Measured Waveforms

Examples of (a) Arc voltage and (b) Injected energy are shown. (Breaking time 20 kA peak)



**Fig. 9** Relationship between Current Crest Value and Arc Energy

The test result relating to the current crest value and the arc energy is shown.

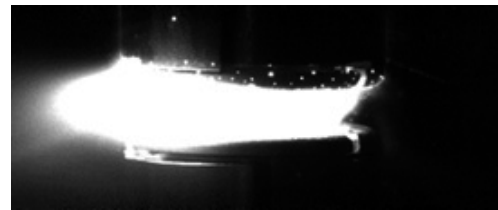
crest value and arc energy and **Table 4** shows the result of comparison of arc energy approximation formulas. **Fig. 10** shows arc images comparison of current crest values.

Judging from **Fig. 9** and **Table 4**, it is recognized that the arc energy decreases as the magnetic field intensity increases. According to **Fig. 10**, we consider that the stronger the magnetic field, the more stabilized the arc mode.

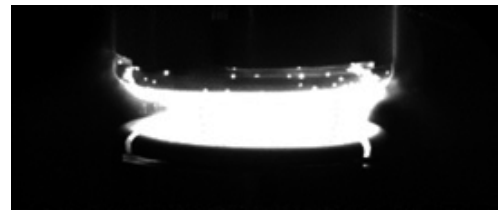
**Table 4** Comparison of Arc Energy Approximation Formulas

An approximate expression of arc energy was derived from the test result.

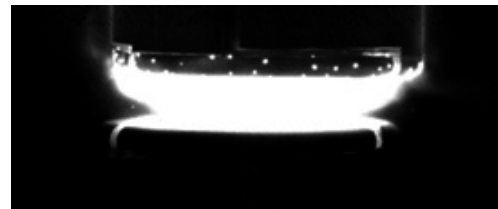
Magnetic field intensity (p.u.)	Approximate expression of arc energy $W = AI_{\text{peak}}^2 + BI_{\text{peak}}$	
	A	B
0.54	$6.442 \times 10^{-6}$	0.1259
0.80	$5.215 \times 10^{-6}$	0.1243
1.00	$4.461 \times 10^{-6}$	0.1240



(a) 0.54 p.u.



(b) 0.80 p.u.



(c) 1.00 p.u.

**Fig. 10** Arc Images Comparison of Current Crest Values

Arc images comparison at a breaking current of 20 kA peak is shown.

### 6.3 Result of Melting Time Measurement

**Fig. 11** shows the result of melting time measurement for the respective AMF electrodes under the modification of the magnetic field intensity and **Fig. 12** shows arc images comparison of current crest values at a magnetic field intensity of 0.54 p.u.

As shown in **Fig. 11**, the melting time tends to be longer when the arc energy is increased. Under the condition of 0.54 p.u., however, the melting time changes its behavior from the former tendency and

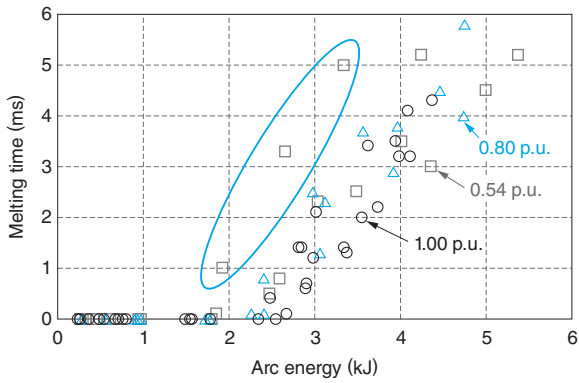
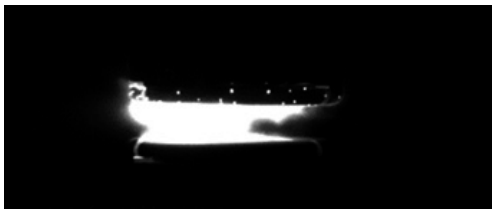
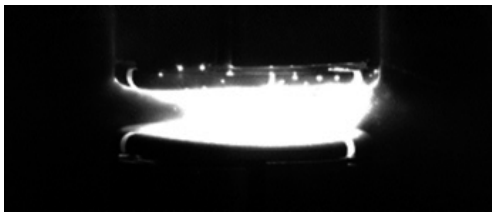


**Fig. 11** Result of Melting Time Measurement

The measuring result from the arc energy and the melting time is shown.



(a) For biased arcs



(b) For spread arcs

**Fig. 12** Arc Images Comparison of Current Crest Values at a Magnetic Field Intensity of 0.54 p.u.

The result of arc images comparison at a magnetic field intensity of 0.54 p.u. is shown.

becomes longer as the result of measurement indicates. Based on the result of comparison of arc images, we found that arcs are biased and locally concentrated when the melting time becomes longer than that of other cases as suggested in Fig. 12.

## 7 Postscript

Using AMF electrodes with different magnetic field intensities, we implemented quantitative evaluation of the relationship between field intensity and arc energy.

According to the result of arc observation and the electrode surface temperature measured after the current-zero point, we noticed that a correlation lies between arc energy and melting time. We also clarified that the melting time tends to be extended when arcs are not spread uniformly. An increase in the electrode melting time is subject to the occurrence of reduction of current interruption capability and withstand voltage performance.

Going forward, we will try to grasp the insulation recovery characteristics by applying a voltage after the current-zero point and clarify the thermal limit for current interruption.

• All product and company names mentioned in this paper are the trademarks and/or service marks of their respective owners.